Article

Fluorescence Amplification by Electrochemically Deposited Silver Nanowires with Fractal Architecture

Ewa M. Goldys, Krystyna Drozdowicz-Tomsia, Fang Xie, Tanya Shtoyko, Eva Matveeva, Ignacy Gryczynski, and Zygmunt Gryczynski

J. Am. Chem. Soc., **2007**, 129 (40), 12117-12122• DOI: 10.1021/ja071981j • Publication Date (Web): 13 September 2007

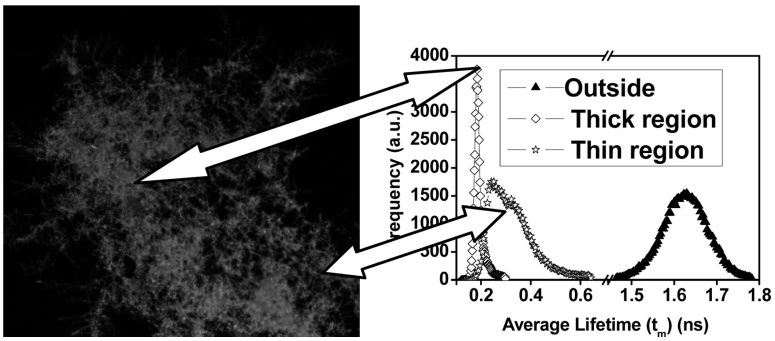

More About This Article

Additional resources and features associated with this article are available within the HTML version:

- Supporting Information
- Links to the 3 articles that cite this article, as of the time of this article download
- Access to high resolution figures
- Links to articles and content related to this article
- Copyright permission to reproduce figures and/or text from this article

View the Full Text HTML

J|A|C|S
ARTICLES
Published on Web 09/13/2007

Fluorescence Amplification by Electrochemically Deposited Silver Nanowires with Fractal Architecture

Ewa M. Goldys,*,† Krystyna Drozdowicz-Tomsia,† Fang Xie,† Tanya Shtoyko,‡ Eva Matveeva,§ Ignacy Gryczynski,§ and Zygmunt Gryczynski§

Contribution from the Macquarie University Biotechnology Research Institute, North Ryde 2109 NSW Australia, University of Texas at Tyler, Tyler, Texas 75799, and Center for Commercialization of Fluorescence Technologies, Health Science Center, University of North Texas, Fort Worth, Texas 76107

Received March 20, 2007; E-mail: goldys@ics.mq.edu.au

Abstract: Electrochemically deposited silver structures with nanowires 50−100 nm in diameter show high fluorescence amplification and strongly reduced fluorescence lifetimes. Both quantities depend on the structure thickness. With increasing thickness the fluorescence amplification proportionally increases and the fluorescence lifetime decreases. This thickness dependence is caused by fluorophore interaction with a system of plasmon excitations in coupled nanowires extending over micrometer size regions. Thus the amplification is attributed to a combination of extended structure area and strong plasmonic coupling between nanowires which also help to radiatively scatter the fluorescence emission.

Introduction

Amplification of fluorescence is a nanoscale phenomenon which is particularly pronounced in close proximity to metal nanostructures. Due to its sharp distance dependence, it is ideally suited to monitor biorecognition reactions. Metal structures have been reported to amplify fluorescence, via a process where the proximity of the metal enhances quantum yield and reduces lifetimes.[1] Earlier fluorescence amplification studies were carried out by using silver colloids immobilized on the glass surface, light-deposited and electroplated silver, roughened silver electrodes, and nanolithographically produced structures.[2−4] Much of recent work was carried out with silver islands deposited by the reduction of silver citrate method.[5] However it is the electrodeposited silver referred to as "fractal-like" which has been reported to produce the highest fluorescence amplification of up to a few hundred.[6,7] The silver coverage in a typical structure is nonuniform, and the amplified fluorescence shows strong nonuniformity, also observed in this work. Parallels can be drawn with surface enhanced Raman scattering and other nonlinear optical effects where intense signals can be observed from isolated "hot spots".[8,9] This paper examines the reasons for such high amplification factors in electrodeposited structures with the aim to identify specific mechanisms of fluorescence enhancement and their respective contributions.

Growth of metallic structures by electrochemical deposition has been one of the most extensively investigated growth processes. In the original diffusion-limited aggregation (DLA) growth model of Witten and Sander[10] particles are added one at a time to a growing aggregate via random walk paths starting outside of the region occupied by the cluster. This model was extensively studied by mathematical simulations, and it has been demonstrated that the internal structure and scaling could be described in terms of fractal dimensionality. This has implications for the analysis of fluorescence amplification, because, in principle, such fractal structures can have a very large (theoretically infinite) surface, which could explain high fluorescence amplification factors for fluorescent monolayers covering such structures.

Experimental Section

Silver structures were prepared in the following fashion.[11] The microscope slides (VWR Scientific) were thoroughly washed with Alconox soap, wiped with isopropanol, and rinsed with distilled water. Two pieces of silver foil (25 mm × 30 mm × 1 mm each) (Sigma-Aldrich) were placed about 25 mm apart between two microscope slides held by tape. The gap between two microscope slides was filled with deionized water (pH 6.4). A direct current of 100 μA was passed between two silver foil electrodes for 20 min, and during that time the

† Macquarie University Biotechnology Research Institute.
‡ University of Texas at Tyler.
§ University of North Texas.

(1) Lakowicz, J. R.; Malicka, J.; Gryczynski, I.; Gryczynski, Z.; Geddes, C. D. *J. Phys. D: Appl. Phys.* **2003**, *36*, 240.
(2) Geddes, C. D.; Cao, H.; Gryczynski, I.; Gryczynski, Z.; Fang, J.; Lakowicz, J. R. *J. Phys. Chem. A* **2003**, *107*, 3443.
(3) Geddes, C. D.; Parfenov, A.; Roll, D.; Gryczynski, I.; Malicka, J.; Lakowicz, J. R. *Spectrochim. Acta A* **2004**, *60*, 1977.
(4) Leveque-Fort, S.; Fort, E.; Le Moal, E.; Lacharme, J. P.; Fontaine-Aupart, M. P.; Ricolleau, C. Proceedings of SPIE-The International Society for Optical Engineering 5327 (Plasmonics in Biology and Medicine), 2004, 29.
(5) Lakowicz, J. R.; Shen, Y.; D'Auria, S.; Malicka, J.; Gryczynski, Z. *Anal. Biochem.* **2002**, *301*, 261.
(6) Parfenov, A.; Gryczynski, I.; Malicka, J.; Geddes, C. D.; Lakowicz, J. R. *J. Phys. Chem. B* **2003**, *170*, 8829.
(7) Geddes, C. D.; Parfenov, A.; Roll, D.; Gryczynski, I.; Malicka, J.; Lakowicz, J. R. *J. Fluoresc.* **2003**, *13*, 267.
(8) Shalayev, V. M.; Botet, R.; Tsai, D. P.; Kovacs, J.; Moskovits, M. *Physica A* **1994**, 197.
(9) Markel, V. A.; Shalayev, V. M.; Stechel, E. B.; Kim, W.; Armstrong, R. L. *Phys. Rev. B* **1991**, *33*, 2425.
(10) Witten, T. A.; Sander, L. M. *Phys Rev Lett* **1981**, *47*, 1400.
(11) Fleury, V.; Watters, W. A.; Allam, L.; Devers, T. *Nature* **2002**, *416*, 716.

voltage typically dropped from 12 V to about 6 V as the structures grew starting from the cathode. After overnight drying the structures were stored in deionized water.

We used two types of fluorescent monolayers, based on FITC labeled HSA which spontaneously binds to glass and silver and can produce complete coverage[12] and a rabbit−antirabbit IgG conjugate. Both types produced closely similar results. The HSA−FITC complex has been selected because the size of the HSA molecule of 4 nm is close to the optimal distance for fluorescence enhancement of the FITC molecules. The conjugate used in this work had nine FITC molecules per one HSA molecule. As these nine FITC molecules are in relatively close proximity, they are subjected to self-quenching which is reflected in the observed average FITC lifetime of 1.6 ns, compared with 4 ns for isolated FITC molecules.[13] The second type of monolayers has been selected for ease of comparison with the earlier literature.[14]

Binding of FITC−HSA to the silvered surface, or to the glass surface (in control experiments), was accomplished by incubating the surfaces in a 10 μM FITC−HSA solution overnight at 4 °C, followed by rinsing with buffer to remove the unbound materials.[15] The deposition of IgG monolayers was carried out following ref 26. First, the slides were exposed to poly-lysine for 1 h and rinsed with water (250 μL of poly-lysine solution with 0.01% poly-L-lysine in 5 mM Na-phosphate buffer, pH 7.3). Further, rabbit IgG was noncovalently immobilized on the slide. This was done by overnight incubation at +4 °C of a solution of 50 μg/mL rabbit IgG in Na-phosphate buffer, at a pH of 7.3. The slides were then thoroughly rinsed with water, 0.05% Tween-20 in water, and water again. Further the surface was blocked with a blocking solution (1% bovine serum albumin, 1% sucrose, 0.05% NaN_3, 0.05% Tween-20 in 50 mM Na-phosphate buffer, pH 7.4, 100 μL/well, 2 h at room temperature) and rinsed again. Further, Rhodamine Red-X labeled antirabbit IgG conjugate (10 μg/mL in blocking solution) was placed on the slide. The slide was then incubated for 1 h at room temperature, rinsed, and covered with 50 mM Na-phosphate buffer.

Simultaneous fluorescence and transmission characterization was carried out using a laser scanning microscope LSM410 (Zeiss) at 488 nm. The measurement of spatially averaged fluorescence spectra used a Varian Cary Eclipse system at 532 nm excitation. Simultaneous fluorescence intensity and lifetime measurements were taken at the same experimental conditions on a Leica SP2 Confocal Fluorescence Microscopy System with Fluorescence Lifetime Imaging (FLIM) based on a Time Correlated Single Photon Counting (SPC-830) module with 256 by 256 channels from Becker and Hickl. The excitation was provided by a 405 nm pulsed laser diode modulated at 40 MHz. The fluorescence signal passing through an Airy pinhole (114 micrometers) was detected by a PMC-100-0 detector from Becker & Hickl which makes it possible to reliably measure minimum lifetimes of 100 ps.[16] The lifetime data were corrected for the instrument response function (IRF). Direct measurement of the IRF requires recording of the laser pulses through the normal optical path of the detection system which is difficult in microscopes because the same beam path is used for the excitation and emission light. Under these conditions the laser light is scattered at multiple optical surfaces inside the microscope, and a clean reflection from the sample plane is usually not obtained. Instead of such a direct method, in the Becker and Hickl system the IRF is estimated from the data trace for each pixel separately by calculating the first derivative of the rising part of the signal and by assuming IRF is a symmetric function of time. The observed signal at each pixel is then fitted to a convolution of the IRF thus obtained and a selected decay model (such as single or multiple exponential).[17]

Before the measurements of the silver fractal structures, the microscope optics were carefully aligned. A silver mirror was placed under the microscope, and it was verified that, under these alignment conditions,a negligible fluorescence signal was detected in the imaging mode and, after correcting for the instrument response function, in the FLIM mode. During measurements of the samples, which have different scattering properties than those of the mirror, the instrument response function was evaluated and accounted for at each pixel in the image, as described earlier, so that in the data shown here the instrument response function has been eliminated. The data acquisition time, laser intensity, size of the imaged area, and spatial resolution were optimized to provide a sufficient number of photons in each channel for reliable lifetime analysis. A minimum number of lifetime components, which gave the best agreement with experimental decay data for individual points, was used for calculation of lifetime components, their distribution, and the FLIM image.

The scanning electron microscopy analysis was carried out using an FEI XL30 environmental system. In such systems samples can be analyzed at high pressures, around 1 Torr which alleviates the specimen charging problem, at the expense of slightly inferior spatial resolution. Consequently, although the studied samples were deposited on glass, it was possible to take data without any carbon coating of the surface.

Results and Discussion

Figure 1a shows a representative laser scanning microscopy image of a silver structure coated with a fluorescent monolayer. The confocal z-stack measurements made it possible to estimate the overall thickness of the structure to be on the order of a few micrometers. The spectral emission characteristics (not shown) for the fluorophores bound to the silver structure and control samples with the same fluorophores bound to clean glass were identical. A dark area at the top of the fluorescence image was selected to estimate the average signal from glass coated with the same fluorescent monolayer. This average signal was used to calculate the fluorescence enhancement of the whole image. Figure 1b shows the corresponding transmission image of the same area of the structure. In this image we observe a varying density of silver with darker areas corresponding to locations where more silver was deposited. The "fractal" character of the silver structures is clearly observed and confirmed by testing the fractal dimension using the "box count" definition. In this approach the image is covered by square boxes that vary in size from 2 to 32 pixels. The number of such boxes, N, and their size s are used to compute the fractal dimension, D:

$$D = \lim_{s\to 0}(-\log(Ns)/\log s) \qquad (1)$$

The fractal dimension of 1.73 has been obtained in the structure shown, in agreement with earlier studies of silver deposition on glass[18] where values between 1.52 and 1.89 have been observed.

All the examined silver structures grown showed high and nonuniform fluorescence enhancement, similar to that observed by Parfenov et al.[6] with selected regions where the fluorescence enhancement factor was as high as 57. These highly intense regions tend to occupy only a small fraction of the structure area. We characterized the nonuniformity of fluorescence by digitally coloring the areas with an enhancement larger than 17 (Figure 1d) and 33 (Figure 1e) by setting the image threshold

(12) Doron, A.; Katz, E.; Willner, I. *Langmuir* **1995**, *11*, 1313.
(13) Lakowicz, J. R.; Malicka, J.; D'Auria, S.; Gryczynski, I. *Anal. Biochem.* **2003**, *320*, 13.
(14) Matveeva, E.; Gryczynski, Z.; Malicka, J.; Gryczynski, I.; Lakowicz, R. J. *Anal. Biochem.* **2004**, *334*, 303.
(15) Xie F.; Baker M.; Goldys E. *J. Phys. Chem. B.* **2006**, *110*, 23085.
(16) http://www.becker-hickl.de/_vti_bin/shtml.dll/leicaman.htm, page 54.
(17) http://www.becker- hickl.de/software/tcspc/softwaretcspcspecial.htm, page 4.
(18) Huth, J. M.; Swinney, H. L.; McCormick, W. D.; Kuhn, A.; Argoul, F. *Phys. Rev. E* **1995**, *51*, 3444.

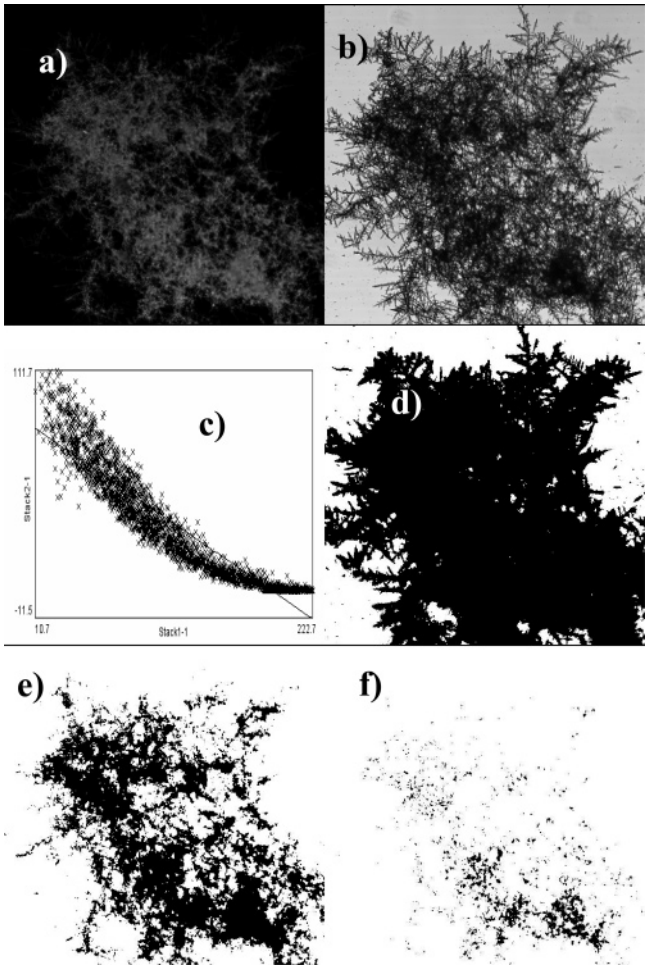

Figure 1. (a) Laser scanning microscopy image of a fluorescent protein monolayer on an electrodeposited silver structure, (b) transmission image of the same region of the structure, and (c) pixel-to-pixel correlation of gray values between the two images. The transmission intensity is displayed on the X axis with the black color corresponding to low readings (near 0) and the white areas of uncovered glass corresponding to high x values, near 255. The fluorescence intensity (Y axis) is displayed in a similar fashion with black near 0 and highly fluorescent regions at high Y values. Linearity improves in the upper left corner where fluorescence is high and transmission low. Saturation is observed on bare glass, not covered with fractals. (d) Regions of the same structure with fluorescence amplification > 1. (e) Regions where fluorescence amplification is >17. (f) Regions with fluorescence amplification > 33. The image size in (a−f) is 170 μm by 170 μm.

at the appropriate values. In these images the dark areas with a magnification of 17 and beyond cover about 30% (Figure 1d), and those with a magnification of 33 and beyond (Figure 1e) cover only 3% of the structure shown.

We have also analyzed the optical transmission image of the structure (Figure 1b) which provides information about the three-dimensional arrangement of the silver structure. This image is characterized by varying gradations of gray with gray values between 0 (black) and 255 (white). The transmission image shows the branches on the periphery of the structure to have a lighter shade of gray, indicating that these outside structures may be comparatively thin. This was later confirmed by ESEM where we observed a 50 nm feature thickness of individual features; at such a thickness silver is partially transparent. The complex, frayed shape of the structure suggests that optical diffraction effects may be significant, especially at the edges. In structures with such loose, uncompacted architecture along the vertical direction the light rays which penetrate deeper into the structure will undergo diffuse reflectance. Consequently, the gradation of gray in the observed transmission image reflects the overall thickness of silver.

Inspection of Figure 1a and 1b strongly suggests that the fluorescence amplification is higher in regions of lower transmission. To examine this further, we calculated the spatial correlation between these images (Figure 1c) which unambiguously shows that high and medium fluorescence intensity and very low/low transmission values are clearly correlated. The saturation shown at the right-hand corner corresponds to those areas of the slide which were not covered by silver. We thus conclude that more substantial silver deposits promote fluorescence amplification, and the effect seems to be gradual. This observation conflicts with the earlier notion of "hot spots"[6] also reported in SERS and theoretically explained by Stockman et al.[19,20] by the effect of special nanostructure arrangement and their close proximity. All the examined structures displayed the same behavior.

To verify whether the structure contains continuous silver deposits, impossible to observe within the limited resolution of optical microscopy, we carried out ESEM studies of our silver structures (Figure 2a,b). Unexpectedly, we found no evidence of layer continuity. The ESEM image shows a loose arrangement of silver nanowires several micrometers in length and with similar radii approximately 50−100 nm in diameter. Within the ESEM depth of focus no continuous silver deposits could be observed, and the deeper layers appear to contain similar nanowires as the layers are closer to the surface. The image on the right shows a magnified image of individual nanowires. At this magnification the depth of focus is smaller, and as the needles have random orientation, a sharp image could not be produced. Assuming the ESEM image is representative of the entire volume of the structure, the surface area can be estimated to be proportional to the thickness of the deposit and to the area density of the nanowires and inversely proportional to the nanowire radius. We also note some shorter and sharp secondary branches protruding sideways from the nanowires which are consistent with the overall fractal architecture of the structure. The image also clearly shows tips of the nanowires, which can act as antennas and effectively emit radiation when coupled to fluorophores.

Given that the silver structures have been produced with the aid of a growth mechanism known to produce fractal shapes, it is understandable that they develop a complex topology with a large number of holes. This is explained within the DLA model where the late arriving particles do not penetrate into the interior of the growing cluster, making it possible for the open architecture to be maintained during growth. This produces an extended surface area oriented in all directions. Although a fraction of fluorophores deposited at such a surface are unable to emit light directly toward the observer, their light may contribute to the overall fluorescence through multiple scattering. Consequently, thicker structures with larger surface areas will produce more fluorescence, although the direct proportionality of fluorescence signal to thickness in very thick structures which significantly obscure light can be challenged.

(19) Stockman, M. I.; Shalaev, V. M.; Moskovits, M.; Botet, R.; George, T. F. *Phys. Rev. B* **1992**, *46*, 2821.
(20) Stockman, M. I.; Bergman, J. D.; Anceau, C.; Brasselet, S.; Zyss, J. *Phys. Rev. Lett.* **2004**, *92*, 57402.

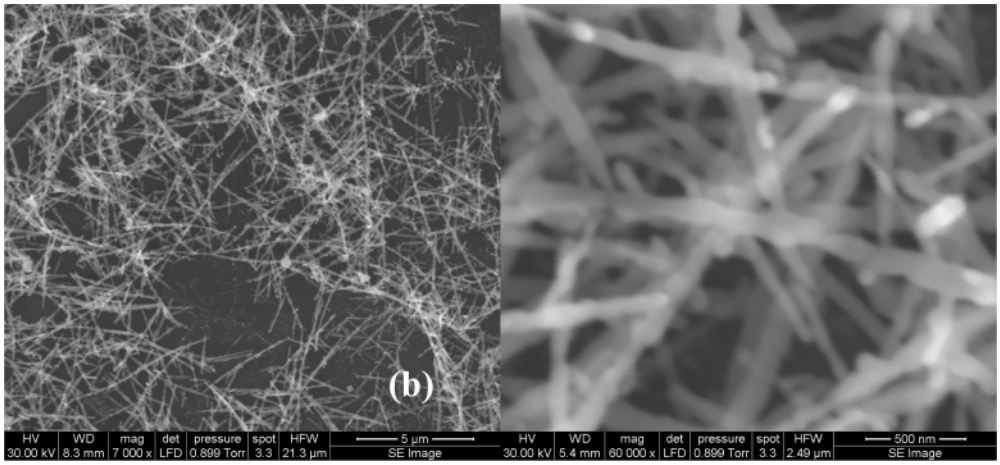

Figure 2. ESEM images of the silver structures: (a) magnification × 7000, bar represents 5 um; (b) magnification × 60000, bar represents 500 nm.

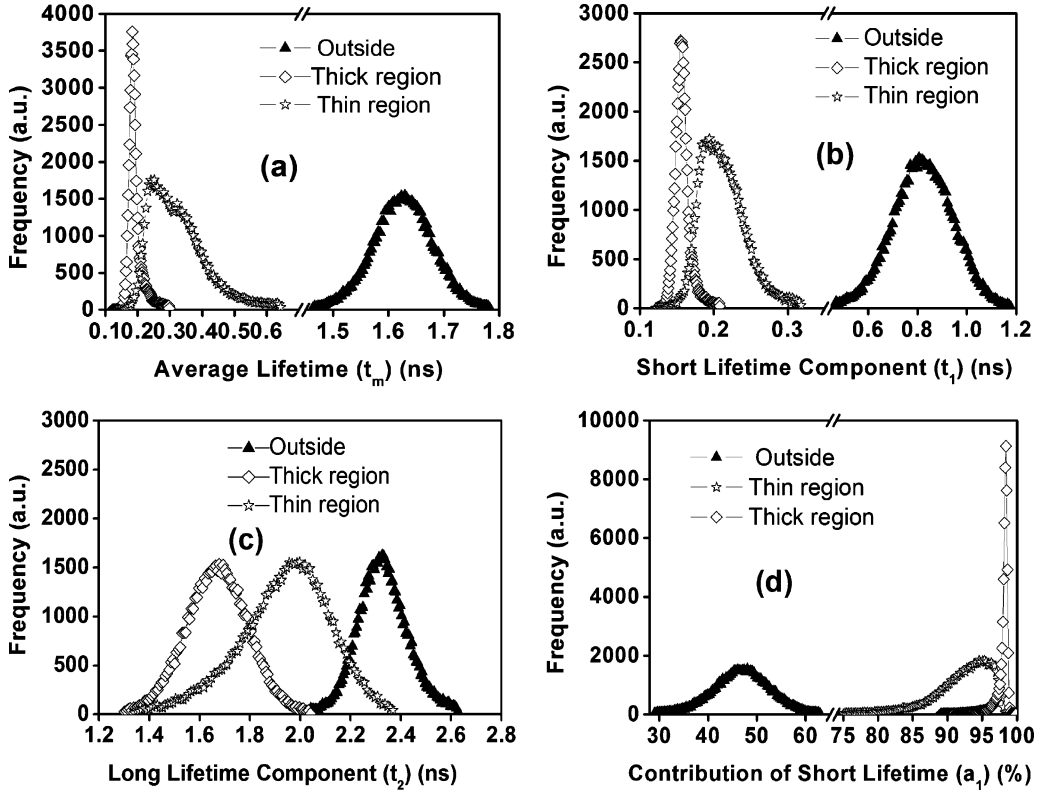

Figure 3. Distributions of parameters obtained in the FLIM data analysis for thick fractal (diamonds), thin fractal (crosses) and control sample with no silver coverage (triangles), (a) average lifetime (b) short lifetime component, t_1, (c) long lifetime component, t_2, (d) contribution of the short lifetime component, a_1.

The explanation of enhanced fluorescence signals by increased surface area and more protein binding in selected spots has been raised by earlier authors.[6] However the conjecture that such an extended surface area is the primary cause for fluorescence amplification needs a separate investigation. To this aim we examined the FLIM images of fluorescent monolayers deposited within the silver structures. We present here the results for two regions: a thin region with dense but visibly discontinuous branches and a thick region which under the optical microscope appeared to contain a dense and continuous silver layer. As a control we used a region outside of the structure where no apparent silver could be observed. The fluorescence decay curves collected in each pixel could be satisfactorily fitted using a model with two decay times t_1 and t_2, from which an average value is calculated using the weighting a_1 and a_2 for each of the decay components

$$I(t) = a_1 e^{-t/t_1} + a_2 e^{-t/t_2} \quad (2)$$

We note that the nonuniformity of the surface over the thickness of about a micrometer seems to cause some weak reflections of the exciting laser pulses; these irregular features were disregarded in the fitting procedure. Each pixel on the image generally showed different values of these parameters, which could be displayed as a map. Figure 3 shows the distributions of calculated values of the average lifetime (t_m), long lifetime component (t_2), short lifetime component (t_1), and contributions to the decay of the short lifetime component (a_1)

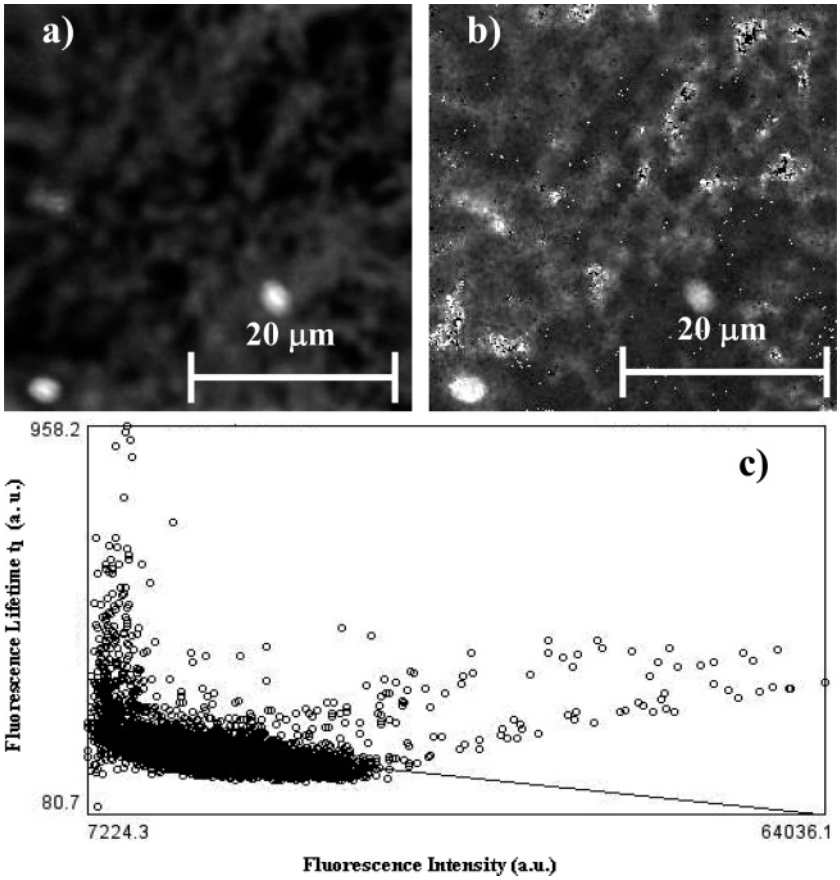

Figure 4. (a) Fluorescence intensity map of the thin fractal. (b) A corresponding map of short lifetime component t_1. (c) Correlation between fluorescence intensity and short lifetime component t_1.

Table 1. Distribution Maxima of the Lifetime Parameters a_1, a_2, t_1, t_2; Error Bars Correspond to FWHM of the Respective Distributions

sample	a_1	a_2	t_1 (ns)	t_2 (ns)
control	0.47 ± 0.11	0.53 ± 0.11	0.80 ± 0.24	2.33 ± 0.18
thin structure	0.95 ± 0.007	0.05 ± 0.007	0.19 ± 0.05	2.0 ± 0.32
thick structure	0.98 ± 0.004	0.02 ± 0.004	0.15 ± 0.01	1.68 ± 0.24

for the investigated region. The contribution of the long lifetime decay (a_2) is not shown as it is complementary to the distribution of a_1. Table 1 shows the maxima for each distribution curve for the three regions.

These results clearly indicate that the fluorescence lifetime for the fluorophores deposited over the silver is significantly reduced, from about 1.6 ns to less than 0.194 ns in thin areas and about 0.155 ns in thick areas. We also emphasize that the short lifetime component t_1 in thin regions is noticeably longer than that in the thick regions.

With the FLIM system response in the order of 30 ps, the observed values are well within the range of our experimental capabilities and accuracy. This is in contrast to an earlier work by Parfenov et al.[6] where an extremely small lifetime value of 3 ps observed for the fluorophores on silver raised the prospect of serious experimental artifacts, such as scattering. We stress however that the effect observed in ref 6, although with fluorophores with much more significant concentration quenching that were equally strong, was a lifetime decrease from 80 to 3 ps. Such a strong decrease of the fluorescence lifetime is consistent with the effect of fluorescence amplification in the proximity of metals.

We also observed (data not shown) that the thick area of the fractal structure is practically dominated by the short lifetime component, while the thin area where both silver and glass regions can be visually observed has some long lifetime contribution. We have also carried out a spatial correlation analysis of long and short decay components for the examined samples and found they also correlate. Moreover, the image of the thin fractal suggests that the lifetimes become smaller close to the middle of the deposits where the thickness increases. This is consistent with our earlier observation that fluorophores in thin fractals show on average longer fluorescence lifetimes than on thick fractals. We thus carried out the correlation analysis between the fluorescence intensity image (Figure 3a) and the FLIM image of the short lifetime component t_1 (Figure 3b). The result (Figure 3c) clearly reveals anticorrelation, which means that higher fluorescence intensity coincides with shorter lifetimes t_1. The reduction in lifetime coupled with an increase in fluorescence intensity is explained by an increase in the radiative decay rate which has been reported in the proximity of metal surfaces (Figure 4).[1,5] This increase of the spontaneous emission rate increases the fluorophore quantum yield while decreasing the lifetime. The effect differs from the influence of the nonradiative rate, whose increase produces a decreased lifetime and decreased quantum yield.

The presented results suggest that the effects of a decreased lifetime and fluorescence amplification in the presence of metal occur gradually and become stronger as the amount of metal in close proximity to the fluorophore increases. This gradual increase can be interpreted as follows. A fluorophore deposited

on a single nanowire couples to this nanowire only so its radiative rate reflects energy transfer to excitations in this single wire. However if the nanowire is surrounded by several more distant nanowires in close proximity, the coupled excitation can extend to these too, thus producing new channels for energy transfer, and, consequently, a further reduced radiative lifetime. Thus the effect of nanowires on the fluorophore depends on how many of them are available to engage in a coupled excitation and, therefore, on the structure thickness. The observed thickness variations of fluorescence intensity and lifetime suggest some differences between thin and thick regions of the structure with respect to these coupled oscillations, and therefore the extent of these coupled oscillations are likely to be on the order of a few micrometers. We should note here that the idea of coupled plasmons in complex metal structures which enhance radiative effects has already found interesting applications elsewhere,[21,22] and it offers further interesting opportunities for engineering of these effects.

The ESEM image of the structure suggests that the high level of fluorescence amplification from this and similar structures can be attributed to several effects. First, the open architecture of the structure in the ESEM image which is consistent with the accepted models of electrodeposition provides the opportunity for fluorescent monolayers to extend over the entire structure possibly in a uniform fashion on all nanowires. This explains the observation that the fluorescence intensity increased with increasing apparent surface density of silver deposits. However the greatly increased total surface area owing to the random stacking of nanowires is not the only factor which contributes to fluorescence amplification. The second factor which contributes to fluorescence enhancement is the high aspect ratio of the nanowires. The electric dipole moment for electron resonance oscillations along such wires is greatly enhanced compared to more spherical nanoparticles, and any coupling of the optical transitions in the fluorophore molecules to these vibrations may result in antenna effects where the coupled radiation is effectively reemitted to free space. Third, the well-established effect of metal enhancement continues to take place as evidenced by the greatly reduced fluorescence lifetime. Other effects such as partially relieved self-quenching[12] and possibly increased excitation rate due to an enhanced electric field also make a contribution. With all these cooperating effects the fluorescence amplification can achieve high values.

Conclusions

In summary we investigated fluorescence amplification in an electrodeposited silver structure with a fractal architecture covered with fluorescent monolayers. They show high (up to 57) and nonuniform fluorescence amplification which is correlated with structure thickness. The nanoscale image reveals stacks of nanowires 50−100 nm in diameter and several micrometers in length, producing an extended surface area. The fluorophore lifetime is greatly decreased in a manner correlated with fluorescence amplification and thus with increasing thickness. These effects are explained by coupled excitation in the nanowires close to a given fluorophore, which are likely to extend over micrometer distances. The nanowires also promote fluorescence amplification in other ways, as with their high aspect ratio and sharp tips they act as antennas for the radiating fluorophores.

On a fundamental physics level the system of fluorophores attached to nanowires with the fractal architecture examined here represents an intermediate case between one extreme of a fluorophore attached to a single isolated spherical nanoparticle — a system where fluorescence amplification is small and the radiative rate is reduced somewhat[2,15] — and another extreme of a solid metal surface where fluorophores are coupled to the entire volume of the metal which reduces the nonradiative rate so much that the fluorescence is quenched. From an application point of view we envisage its applications as a fluorescence-amplifying bioassay platform with a greatly extended surface owing to the small wire diameter and their arrangement.

Acknowledgment. This project was partially funded by the ARC DP0770902 and RN0460002.

JA071981J

(21) Barnett, A.; Matveeva, E.; Gryczynski, Z.; Gryczynski, I.; Goldys, E. M. *Physica B* **2007**, *394*, 297.
(22) Song, J. H.; Atay, T.; Shi, S.; Urabe, H.; Nurmikko, A. V. *Nano Lett.* **2005**, *5*, 1557.